Article

# The Voltage Activation of Cortical KCNQ Channels Depends on Global PIP2 Levels

Kwang S. Kim,[1] Kevin M. Duignan,[1] Joanna M. Hawryluk,[1] Heun Soh,[1] and Anastasios V. Tzingounis[1,*]
[1]Department of Physiology and Neurobiology, University of Connecticut, Storrs, Connecticut

ABSTRACT The slow afterhyperpolarization (sAHP) is a calcium-activated potassium conductance with critical roles in multiple physiological processes. Pharmacological and genetic data suggest that KCNQ channels partly mediate the sAHP. However, these channels are not typically open within the observed voltage range of the sAHP. Recent work has shown that the sAHP is gated by increased $PIP_2$ levels, which are generated downstream of calcium binding by neuronal calcium sensors such as hippocalcin. Here, we examined whether changes in $PIP_2$ levels could shift the voltage-activation range of KCNQ channels. In HEK293T cells, expression of the PIP5 kinase PIPKI$\gamma$90, which increases global $PIP_2$ levels, shifted the KCNQ voltage activation to within the operating range of the sAHP. Further, the sensitivity of this effect on KCNQ3 channels appeared to be higher than that on KCNQ2. Therefore, we predict that KCNQ3 plays an essential role in maintaining the sAHP under low $PIP_2$ conditions. In support of this notion, we find that sAHP inhibition by muscarinic receptors that increase phosphoinositide turnover in neurons is enhanced in *Kcnq3*-knockout mice. Likewise, the presence of KCNQ3 is essential for maintaining the sAHP when hippocalcin is ablated, a condition that likely impairs $PIP_2$ generation. Together, our results establish the relationship between $PIP_2$ and the voltage dependence of cortical KCNQ channels (KCNQ2/3, KCNQ3/5, and KCNQ5), and suggest a possible mechanism for the involvement of KCNQ channels in the sAHP.

## INTRODUCTION

Hippocampal pyramidal neurons express a number of distinct calcium-dependent potassium channels, including calcium-activated large-conductance, small-conductance (SK), and slow afterhyperpolarization (sAHP) potassium channels (1). Although all three of these families have important physiological functions, the sAHP is associated with critical neurological processes, including the acquisition and retrieval of memory (2,3). Additionally, loss of the sAHP correlates with the transition from frequent isolated bursts to continuous firing that is observed in neurological disorders such as epilepsy (4).

Unlike other calcium-activated potassium channels, the sAHP is gated primarily in response to increases in global cytosolic calcium and, in turn, translocation of the neuronal calcium sensors hippocalcin (Hpca) and/or neurocalcin $\delta$ from the cytoplasm to the plasma membrane (5–7). Recent studies suggested that this signaling leads to increased levels of $PIP_2$, which likely acts as the gating entity of the sAHP (8). Studies using genetically altered mice have implicated several KCNQ channels (KCNQ2/3/5) as possible candidates for mediating the sAHP in different cell types (1). All KCNQ channels are gated by $PIP_2$, and thus their probability of opening depends on the concentration of $PIP_2$ in the plasma membrane (9). However, the different KCNQ channel isoforms exhibit a spectrum of $PIP_2$ affinities, with KCNQ3 having the highest and KCNQ2 one of the lowest (10–13).

Despite data suggesting that they play a role in the sAHP, KCNQ channels are not typically active at membrane potentials at which the sAHP is robustly active (i.e., −60 to −70 mV). Therefore, it is currently puzzling how KCNQ channels could underlie the sAHP. Recent findings suggest a possible resolution to this conundrum. An additional conserved $PIP_2$-binding site was identified in KCNQ2 channels at the interface between the voltage sensor and the pore domain (S4-S5 linker), a region critical for electrocoupling (14). Thus, in addition to regulating the open probability of KCNQ2/3/5 channels, $PIP_2$ may also directly regulate their voltage sensitivity, and possibly shift their voltage-activation relationship to within the operating range of the sAHP.

Here, we describe a series of experiments showing that elevating global $PIP_2$ levels in HEK293T cells drives the voltage sensitivity of KCNQ channels to within the operating range of the sAHP. Importantly, the effects of $PIP_2$ persisted in the presence of $\beta$-secretase 1 (BACE1), a recently identified auxiliary KCNQ subunit that leads to an elevated probability of opening (15). Additionally, we showed that this $PIP_2$-induced shift in voltage-dependence sensitivity may be higher in KCNQ3 channels than in KCNQ2 channels. Consistent with this possibility, ablation of KCNQ3 channels led to greater sAHP sensitivity to $PIP_2$ turnover (via muscarinic G-protein-coupled receptor (GPCR) activation or

*Submitted July 21, 2015, and accepted for publication January 13, 2016.*
*Correspondence: anastasios.tzingounis@uconn.edu
Kwang S. Kim and Kevin M. Duignan contributed equally to this work.
Editor: William Kobertz.

0006-3495/16/03/1089/10
http://dx.doi.org/10.1016/j.bpj.2016.01.006

reduced $PIP_2$ generation in Hpca-deficient mice). These results establish the relationship between $PIP_2$ and the voltage dependence of KCNQ channels, and suggest a mechanism for the involvement of KCNQ channels in the sAHP.

## MATERIALS AND METHODS

Experiments were carried out in accordance with the guidelines of the University of Connecticut-Storrs Institutional Animal Care and Use Committee.

### Animals and genotyping

Both male and female mice were used for slice physiology experiments. *Kcnq3* germline knockout mice were generated by crossing *Kcnq3*-flox (*Kcnq3*$^{fl/fl}$) mice to *Hprt*-cre mice (http://jaxmice.jax.org/strain/004302.html). The *Kcnq3*$^{fl/fl}$*:Hprt*-cre mice were then further bred to remove the *Hprt*-cre cassette. *Hippocalcin* (*Hpca*)-knockout mice were generated as described previously (5). *Hpca*$^{-/-}$*:Kcnq3*$^{-/-}$-knockout mice were generated by intercrossing *Hpca*$^{+/-}$*:Kcnq3*$^{+/-}$. Although the *Hpca*$^{-/-}$ and *Kcnq3*$^{-/-}$ mice survived to adulthood and showed no evidence of seizures, the majority of double *Hpca*$^{-/-}$*:Kcnq3*$^{-/-}$ mice died by the second to third week of life. Additionally, on multiple occasions we noted that these mice underwent tonic-clonic seizures. These phenotypes suggest a negative epistasis between *Hpca* and *Kcnq3*. PIPKI$\gamma$ heterozygous mice (http://jaxmice.jax.org/strain/023815.html) were obtained from The Jackson Laboratories. All genetic strains were maintained on a C57Bl/6 background. PCR genotyping of mouse-tail prep DNA was performed using the following primers: *PipkI*$\gamma$, 5′-CCTCACATCCTGCTCACTCAGGACC-3′, 5′-GCCTCACAGAGATTTGACGTGTCAG-3′, 5′-CACCCCTTCCCAGCCTCTGA-3′; *Kcnq3*, 5′-TCCACTTCCATGTTCAATGC-3′, 5′-CAGCACTCCCATGACAAATG-3, 5′-TCTCCCATGGCAAGTATTCC-3; and *Hpca*, 5′-ACTGGCTCCTCAGCCTTTGTCTCTGAACAC-3′, 5′-TCGTGCTTTACGGTATCGCCGCTCCCGATT-3′, 5′-TAGCCAGAGCTATGTAGTGAGATCCTGTCTC-3′.

### Slice preparation and electrophysiology

Transverse hippocampal slices (300 $\mu$m) were prepared from 10- to 19-day-old mice. The animals were deeply anesthetized with isoflurane and then immediately decapitated. The brain was rapidly dissected out and placed in ice-cold cutting solution containing (in mM) 26 $NaHCO_3$, 210 sucrose, 10 glucose, 2.5 KCl, 1.25 $NaH_2PO_4$, 0.5 $CaCl_2$, and 7 $MgCl_2$. The hippocampus was then glued to the stage of a Microm vibroslicer immersed in cutting solution and sliced. The slices were placed in a storage chamber filled with artificial cerebrospinal fluid (ACSF, in mM: 119 NaCl, 2.5 KCl, 1.3 $MgCl_2$, 2.5 $CaCl_2$, 1 $NaH_2PO_4$, 26 $NaHCO_3$, and 10 glucose) continuously bubbled with 95% $O_2$ and 5% $CO_2$. The slices were maintained at 35°C for 30–40 min and then at room temperature for at least 1 h before recordings were obtained. All experiments were performed at room temperature. During recordings, slices were continuously perfused in ACSF with the addition of 2 $\mu$M CNQX to block fast synaptic transmission.

Hippocampal pyramidal neurons were visually identified with infrared differential interference contrast optics using a 40× water-immersion objective lens on an upright microscope (model No. BX51W; Olympus, Melville, NY). Whole-cell recordings were obtained using electrodes pulled from thin-walled borosilicate glass capillaries (World Precision Instruments, Sarasota, FL) with a resistance of 3.5–5 MΩ and filled with an intracellular solution consisting of (in mM) 130 potassium methylsulfate, 10 KCl, 10 HEPES, 4 NaCl, 4 $Mg_2ATP$, 0.4 $Na_4GTP$, and 20 myo-inositol. The osmolarity was adjusted to 295–300 mOsm and the pH was adjusted to 7.25–7.35 with KOH. All slice recordings were taken from pyramidal neurons located in the CA3 region of the hippocampus with an initial resting membrane potential of $<-55$ mV (not junction potential corrected). All recordings were performed through a Multiclamp 700B amplifier (Molecular Devices, Sunnyvale, CA), filtered at 2 kHz, and sampled at 10 kHz. Data were analyzed offline using Axograph X (Axograph, Queensland, Australia), Clampfit (Molecular Devices, Sunnyvale, CA), or IgorPro (WaveMetrics, Lake Oswego, OR) software. The series resistance was measured by the instantaneous current response to a 4 mV (100 ms) step pulse with only the pipette capacitance canceled out. The series resistance was measured continuously and recordings were discarded if it changed by >20%. Recordings were not adjusted for the calculated junction potential (−8.6 mV). For all slice recordings, the membrane potential was clamped to −55 mV.

### HEK293T electrophysiology

HEK293T cells were transfected with recombinant DNA (3–5 $\mu$g) using Lipofectamine 2000 (Invitrogen, Carlsbad, CA) and recorded 2 days after transfection. All experiments were performed at room temperature using conventional whole-cell patch-clamp electrophysiology. The recording electrodes had a resistance of 3–6 MΩ and were filled with an internal solution containing (in mM) 132 K-gluconate, 10 KCl, 4 Mg·ATP, 20 HEPES, and 1 EGTA·KOH, pH 7.2–7.3. To avoid rapid rundown of the KCNQ current during the whole-cell patch-clamp recordings, we used an intracellular solution that contained 1 mM EGTA (rather than the widely used 10 mM concentration; in our experience, concentrations of calcium chelators above 1 mM lead to a very rapid diminution of KCNQ currents). The extracellular bath solution contained (in mM) 144 NaCl, 2.5 KCl, 2.25 $CaCl_2$, 1.2 $MgCl_2$, 10 HEPES, and 22 D-glucose, pH 7.2–7.3. The series resistance was 75% compensated. The osmolarity was adjusted to 300–305 mOsm and the pH was adjusted to 7.2–7.3 with NaOH. Voltage pulses were applied at 30 s intervals from a holding potential of −70 mV to various test pulses before jumping down to −55 mV, as described in the figure legends. Values reported in each figure were adjusted for the calculated junction potential (−15 mV). Data were acquired through a Multiclamp 700B amplifier (Molecular Devices), low-pass filtered at 2 kHz, and sampled at 20 kHz. Analysis of the data was accomplished using Clampfit (Molecular Devices) and IgorPro (WaveMetrics) software.

### Constructs

All KCNQ channel constructs used in this study have been described previously (16). The PIPKI$\gamma$90 plasmid was kindly provided by Dr. R. Irvine (Cambridge University) and subsequently subcloned into an IRES-dsRed plasmid. The Ci-VSP-GFP construct was kindly provided by Dr. Y. Okamura (Osaka University) and the BACE1 construct was provided by Drs. C. Alzheimer and T. Huth (Friedrich-Alexander Universität Erlangen-Nürnberg).

### Drugs and reagents

Chemical reagents were purchased from Sigma-Aldrich (St. Louis, MO), with the exception of apamin and CNQX (Abcam, Cambridge, MA), and retigabine (Santa Cruz Biotechnologies, Santa Cruz, CA; Alomone Labs, Jerusalem, Israel). Dulbecco's modified Eagle's medium, minimal essential medium, penicillin, streptomycin, and fetal calf serum were purchased from Invitrogen (Carlsbad, CA).

### Data analysis and statistics

We used the built-in algorithms of Clampfit (Molecular Devices) and IgorPro (Wavemetrics) to obtain the Boltzmann and exponentials fits of our data. Data are displayed as means ± SEM, and significance was determined by two-way Student's *t*-test or one-way ANOVA using the built-in algorithms of KaleidaGraph 4 (Synergy Software, Reading, PA) and Prism (Graphpad Software, La Jolla, CA).

## RESULTS

### Increased $PIP_2$ levels shift the voltage activation of KCNQ channels to more negative potentials

To test whether $PIP_2$ directly regulates the voltage sensitivity of KCNQ channels, we probed the effect of altered $PIP_2$ levels on the voltage-activation properties of KCNQ channels expressed in HEK293T cells. Previous work has shown that overexpressing PIPKIγ90, the major $PIP_2$-synthesizing enzyme in the brain, leads to significant increases in plasma membrane $PIP_2$ levels in cultured cells (12,17). Therefore, we compared the voltage-activation properties of KCNQ2/3 in the presence and absence of PIPKIγ. We chose this heteromeric channel combination because KCNQ2/3 channels are the primary KCNQ channels in pyramidal neurons (18). We also examined KCNQ3/5, KCNQ5, and KCNQ3 channels, which may also be expressed by these neurons.

HEK293T cells transfected with either KCNQ2/3 or KCNQ3/5 produced outward currents after 1 s depolarization steps, consistent with previous studies (Fig. 1, *ai* and *aii*) (19). To determine the half-activation voltage of the expressed KCNQ channels, we returned the membrane potential to −70 mV after each depolarization step. The resulting

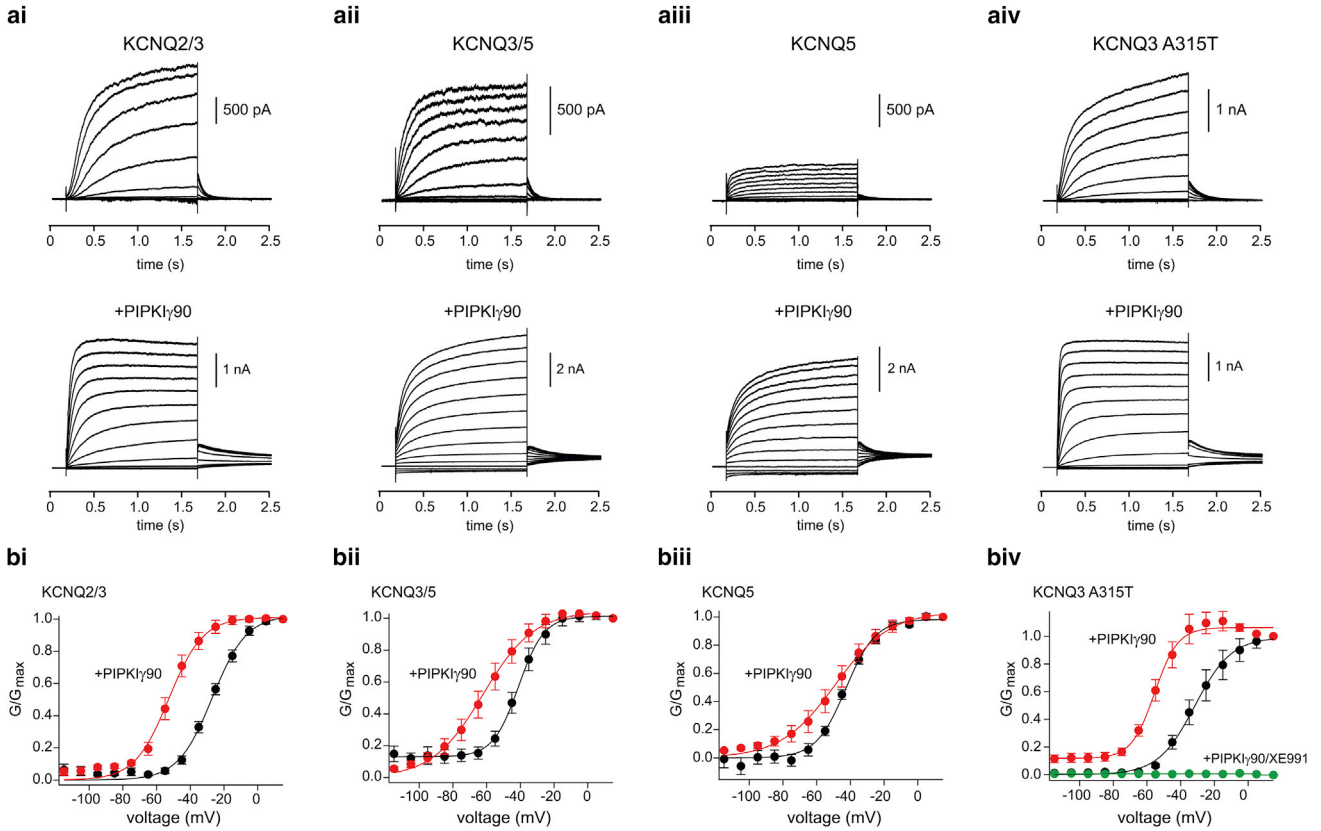


FIGURE 1 $PIP_2$ regulates the voltage-activation properties of neuronal KCNQ channels. (*a*) Representative current traces at different membrane potentials from HEK293T cells expressing (*i*) KCNQ2/3, (*ii*) KCNQ3/5, (*iii*) KCNQ5, or (*iv*) $KCNQ3^{A315T}$ alone (*top panel*) or in the presence of PIPKIγ90 (*bottom panels*). For these experiments, KCNQ currents were measured at various test potentials elicited by a 1 s depolarization from −85 mV, followed by a return step to −70 mV. Test potentials ranged from −115 mV to +15 mV in 10-mV increments. (*b*) Normalized G-V relationship to the maximum tail current at −70 mV for (*i*) KCNQ2/3 ($n = 8$, +PIPKIγ90 $n = 6$), (*ii*) KCNQ3/5 ($n = 7$, +PIPKIγ90 $n = 6$), (*iii*) KCNQ5 ($n = 10$, +PIPKIγ90 $n = 5$), or (*iv*) $KCNQ3^{A315T}$ ($n = 5$, +PIPKIγ90 $n = 5$). Data represent mean ± SEM. Note that there was a large increase in the current responses in KCNQ5-containing cells when coexpressed with PIPKIγ90. For instance, in the absence of PIPKIγ90 the KCNQ3/5 and KCNQ5 current responses at +15 mV were 921 ± 238 pA ($n = 7$) and 510 ± 38 pA ($n = 10$), respectively, whereas in the presence of PIPKIγ90 they were 8141 ± 1088 pA ($n = 6$) and 3416 ± 747 pA ($n = 5$). In addition to shifting the voltage activation of $KCNQ3^{A315T}$ channels to the left, PIPKIγ90 induced constitutive voltage-independent activity of $KCNQ3^{A315T}$ (~15%) (*iv*). We verified that this basal activity occurred through $KCNQ3^{A315T}$ channels, as application of the selective KCNQ blocker XE991 (20 μM) completely eliminated it. Coexpression of KCNQ3/5 seemed to give rise to a small (~10%) voltage-independent current. However, and in contrast to the data obtained for $KCNQ3^{A315T}$, we could not verify that this current flows through KCNQ3/5 channels, as application of 40 μM XE991 did not affect its amplitude at hyperpolarized membrane potentials (at −75 mV: 17 ± 1 pA; +XE991 16 ± 2 pA, $n = 4$). Elevated $PIP_2$ levels led to slower deactivation of the tail current in the presence of PIPKIγ90. For instance, after a step from −35 mV, the deactivation time constant of KCNQ2/3 at −70 mV was 51 ± 7 ms ($n = 8$) and 167 ± 44 ms ($n = 6$; $p < 0.05$) in the presence and absence of PIPKIγ90, respectively. We found similar changes for KCNQ3/5 channels (KCNQ3/5, $\tau = 127 \pm 29$ ms, $n = 7$ $\tau_{PIPKI\gamma} = 231 \pm 17$ ms, $n = 6$, $p < 0.05$ Student's *t*-test), but not KCNQ5 channels ($\tau = 140 \pm 26$ ms, $n = 10$, $\tau_{PIPKI\gamma} = 166 \pm 7$ ms, $n = 5$; $p = 0.5$ Student's *t*-test). To see this figure in color, go online.

tail current allowed us to construct a conductance-to-voltage (G-V) relationship (17). Fig. 1 *a* shows representative examples of families of KCNQ-mediated traces at different membrane potentials. On average, KCNQ2/3 and KCNQ3/5 currents activated with a midpoint voltage ($V_{0.5}$) of $-27 \pm 1.3$ mV ($n = 8$) and $-40 \pm 2.1$ mV ($n = 7$) (Fig. 1, *bi* and *bii*), respectively, whereas cells expressing KCNQ5 channels activated with a $V_{0.5}$ of $-43 \pm 2.4$ mV ($n = 10$) (Fig. 1 *biii*). We also studied KCNQ3-mediated currents using $KCNQ3^{A315T}$ mutant channels, which give more robust currents in heterologous cells than wild-type channels. The voltage-dependent and $PIP_2$ properties of $KCNQ3^{A315T}$ channels ($V_{0.5}$ of $-35 \pm 1.8$ mV, $n = 5$) are comparable to those of wild-type KCNQ3 channels (Fig. 1, *aiv* and *biv*) (10,20).

We next tested whether cotransfection of KCNQ channels with PIPKIγ could alter KCNQ voltage dependence in HEK293T cells. We found that coexpression of PIPKIγ drove the voltage-activation relationship to more negative membrane potentials for all examined KCNQ channels (KCNQ2/3 $V_{0.5}$: $-52 \pm 2.2$ mV, $n = 6$; KCNQ3/5 $V_{0.5}$: $-62 \pm 4.6$ mV, $n = 6$; KCNQ5 $V_{0.5}$: $-54 \pm 6.3$ mV, $n = 5$; $KCNQ3^{A315T}$ $V_{0.5}$: $-54 \pm 2.5$ mV, $n = 5$; Fig. 1, *bi–iv*). Interestingly, when we fitted the G-V curves with a Boltzmann equation, we found that an increase in $PIP_2$ drove the slope factor to higher values in KCNQ5-containing channels, reflecting a shallower G-V relationship (KCNQ5 slope factor from $8.8 \pm 0.8$, $n = 10$, to $13 \pm 1.6$, $n = 5$, $p < 0.05$; KCNQ3/5 slope factor from $7.7 \pm 0.7$, $n = 7$, to $14 \pm 1$, $n = 6$, $p < 0.001$). This was not the case for KCNQ2/3 or $KCNQ3^{A315T}$ homomeric channels (KCNQ2/3 slope factor from $10 \pm 0.9$, $n = 8$, to $10 \pm 1.5$, $n = 12$, $p = 1$; $KCNQ3^{A315T}$ slope factor from $9.5 \pm 0.8$, $n = 5$, to $7 \pm 1$, $n = 5$, $p = 0.14$).

We also observed that the deactivation kinetics of KCNQ2/3 and $KCNQ3^{A315T}$ were slowed in the presence of PIPKIγ, suggesting that PIPKIγ favors the opening of these channels (see the Fig. 1 legend). Although we did observe altered activation kinetics, we did not systematically quantify these measures. Because the KCNQ activation kinetics reflect several independent processes, they are difficult to interpret and require multiple exponentials to fit the data (21,22). In contrast, PIPKIγ did not alter the deactivation kinetics of KCNQ5 or KCNQ3/5 currents. Instead, PIPKIγ exerted a strong effect on the amplitude of KCNQ5 and KCNQ3/5 currents, producing a sixfold and a nearly ninefold change, respectively (Fig. 1, *aii* and *aiii*). We did not see any difference in capacitance between control cells and those expressing PIPKIγ.

Recent work demonstrated that some KCNQ2/3 and KCNQ5 channels in hippocampal pyramidal neurons are partnered with an auxiliary subunit, BACE1, whose main function is to control protein stability and open probability with minimal effects on voltage dependence (15). As such, we also tested whether elevating $PIP_2$ shifted the G-V relationship of KCNQ2/3 and KCNQ5 channels when coexpressed with BACE1 (Fig. 2). We found that in cells coexpressed with BACE1, $PIP_2$ could still drive the KCNQ2/3 and KCNQ5 G-V relationship to more hyperpolarized membrane potentials (KCNQ2/3 $V_{0.5}$: $-53 \pm 1.7$ mV, slope factor $7.3 \pm 0.5$, $n = 10$; KCNQ5 $V_{0.5}$: $-67 \pm 2.2$ mV, slope factor $11 \pm 2.8$, $n = 3$). Taken together, these data suggest that changes in $PIP_2$ levels can not only affect the KCNQ channel open probability but also shift the voltage activation, thereby allowing KCNQ channels to open at a much larger range of hyperpolarized membrane potentials than has been previously reported.

## $PIP_2$ depletion shifts the voltage activation of KCNQ channels in a subtype-selective manner

Our results indicating that $PIP_2$ regulates the G-V relationship of multiple KCNQ channels are similar to previous findings for KCNQ2/3 (17) and KCNQ2 channels (14). However, this is in contrast to previous work using depletion approaches (23,24). This incongruity could be explained if basal $PIP_2$ levels were low in HEK293T cells. In this case, it would be relatively easy to enhance $PIP_2$ levels by PIPKIγ expression, but more difficult to significantly reduce $PIP_2$ levels through depletion. If $PIP_2$-binding sites are not saturated in KCNQ2/3 channels under basal conditions, we would expect to find little change in their G-V relationship

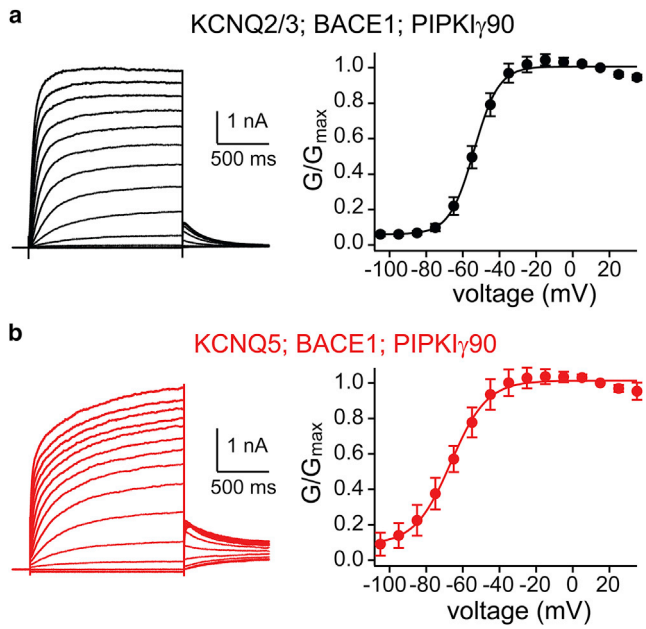


FIGURE 2 $PIP_2$ regulates the voltage-activation properties of neuronal KCNQ channels in the presence of BACE1. (*a*) Left: representative current traces at different membrane potentials from HEK293T cells coexpressing KCNQ2/3, PIPKIγ90, and BACE1 ($n = 10$). Right: normalized G-V relationship to the maximum tail current at $-70$ mV. (*b*) Left: representative current traces at different membrane potentials from cells coexpressing KCNQ5, PIPKIγ90, and BACE1 ($n = 3$). Right: normalized G-V relationship to the maximum tail current at $-70$ mV. Data represent mean ± SEM. To see this figure in color, go online.

in $PIP_2$-depleted conditions. In contrast, $KCNQ3^{A315T}$ channels, which have a high affinity for $PIP_2$, should have a higher occupancy of the $PIP_2$-binding sites under basal conditions. This would be consistent with their typically more negatively shifted G-V curves. Thus, $KCNQ3^{A315T}$, but not KCNQ2/3, channels would exhibit a G-V shift upon depletion of $PIP_2$.

To test this possibility directly, we compared the effects of reducing $PIP_2$ levels on the G-V curve of $KCNQ3^{A315T}$ and KCNQ2/3 channels. We depleted $PIP_2$ by cotransfecting HEK293T cells with either $KCNQ3^{A315T}$ or KCNQ2/3 together with Ci-VSP, a voltage-activated $PIP_2$ phosphatase that strongly depletes $PIP_2$ when activated by extremely depolarized membrane potentials (25). We depolarized cells to −20 mV to measure basal KCNQ current activity, stepped to +105 mV for 4 s to fully activate Ci-VSP, and then returned to −20 mV to again measure the amplitudes of KCNQ currents after $PIP_2$ depletion (Fig. 3 *a*). After the strong depolarization that activates Ci-VSP, $PIP_2$ depletion lasts for several seconds, allowing the measurement of KCNQ-mediated currents under depleted $PIP_2$ conditions.

We also included a voltage-ramp sweep (2 mV/s; from −100 mV to +25 mV) in our protocol, either soon after the step to −20 mV (2) or after 16 s, at which time the $PIP_2$ levels had recovered. The ramp protocol was necessary to obtain a G-V relationship in a short period, avoiding significant changes to $PIP_2$ levels during the protocol. As shown in Fig. 3 *b*, we found that the G-V curve of $KCNQ3^{A315T}$ shifted to more depolarized potentials in the absence of $PIP_2$ ($\Delta V_{0.5} = -6.8 \pm 2.1$, $n = 5$; $p < 0.05$), in contrast to that of KCNQ2/3 channels ($\Delta V_{0.5} = -0.68 \pm 1.5$, $n = 4$; $p = 0.68$). Thus, we conclude that $PIP_2$ depletion can indeed shift the G-V relationship of KCNQ channels, but this depends on their $PIP_2$ occupancy under basal conditions. The rightward G-V shift in the high-affinity $KCNQ3^{A315T}$ channels after $PIP_2$ depletion suggests that they have at least some $PIP_2$ occupancy in binding sites that regulate their voltage dependence under basal conditions. In contrast, the absence of a G-V shift in the lower-affinity KCNQ2/3 channels is likely due to a lower $PIP_2$ occupancy of similar binding sites in KCNQ2/3 channels. We attempted to carry out similar experiments for KCNQ3/5 channels, but the small magnitude of their currents under $PIP_2$-depleted conditions prevented us from accurately measuring voltage ramps.

Using similar experiments, we measured the effect of $PIP_2$ depletion on KCNQ current amplitudes and their time course of recovery from $PIP_2$ depletion. As before, we transfected KCNQ channels with Ci-VSP, carried out the same Ci-VSP activation protocol, and measured KCNQ currents after the return to −20 mV. Under these $PIP_2$-depleted conditions, $KCNQ3^{A315T}$ currents were reduced 61.3% ± 5.1% ($n = 5$), KCNQ2/3 currents were reduced 85.3% ± 2.5% ($n = 4$), and KCNQ3/5 currents were reduced 81.7% ± 3.6% ($n = 3$) (Fig. 4). The time course of $KCNQ3^{A315T}$ current recovery after depletion ($\tau = 3.06 \pm 0.46$ s, $n = 5$) was much faster than the time course for either KCNQ2/3 ($\tau = 8.5 \pm 1.7$ s, $n = 4$) or KCNQ3/5 currents ($\tau = 9.5 \pm 0.6$ s, $n = 3$). Therefore, $KCNQ3^{A315T}$ and (likely) KCNQ3 channels are more resistant to $PIP_2$ depletion and have a faster recovery after depletion.

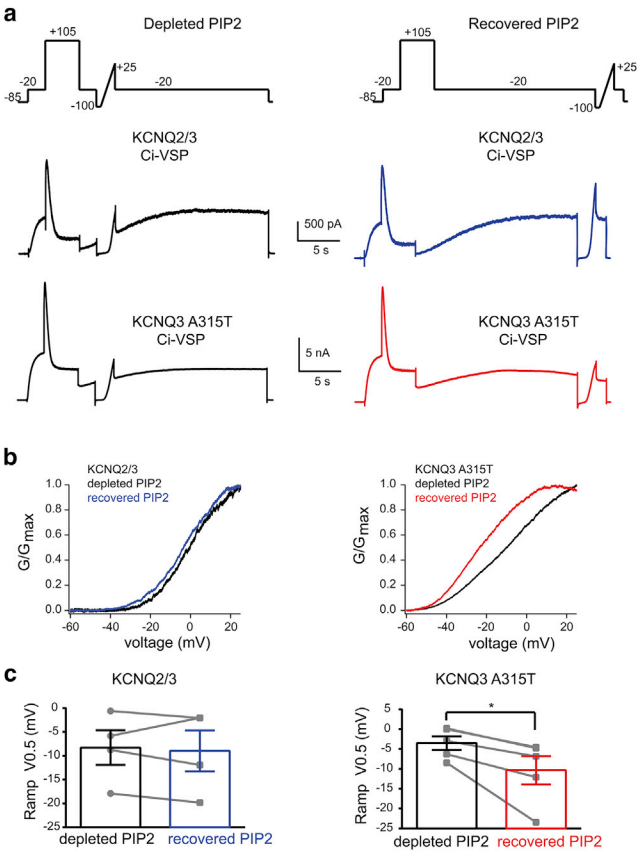


FIGURE 3 $PIP_2$ depletion shifts the voltage activation of KCNQ3 channels to more depolarized membrane potentials. (*a*) Experimental protocol and representative traces from cells coexpressing either KCNQ2/3 or $KCNQ3^{A315T}$ and Ci-VSP. (*b*) Representative G-V relationship of KCNQ2/3 and $KCNQ3^{A315T}$ channels under depleted and recovered $PIP_2$ conditions. (*c*) Summary of KCNQ $V_{0.5}$ under depleted and recovered conditions ($KCNQ3^{A315T}$ $n = 5$; KCNQ2/3 $n = 4$). Data represent mean ± SEM. *$p < 0.05$ using the ANOVA Tukey post hoc test. To see this figure in color, go online.

## KCNQ3 channels are critical for the pyramidal neuron sAHP current under low $PIP_2$ levels

Our heterologous experiments showed that increased levels of $PIP_2$ allowed any cortical KCNQ channel to activate within the sAHP operating age. However, as KCNQ3 channels exhibit a higher affinity for $PIP_2$ (10–13), we predicted that KCNQ3-containing channels might play a greater role in the sAHP under reduced $PIP_2$ conditions. To test this hypothesis, we measured the sAHP current (IsAHP) under two likely $PIP_2$-depleted conditions and examined the effect of genetically ablating *Kcnq3*.

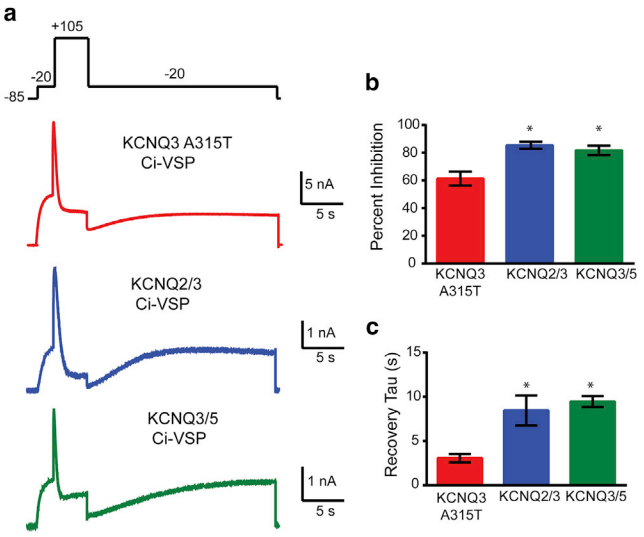


FIGURE 4 KCNQ3 channels are less sensitive to $PIP_2$ depletion. (*a*) Experimental protocol and representative traces from cells expressing $KCNQ3^{A315T}$, KCNQ2/3, or KCNQ3/5 along with Ci-VSP. (*b*) Summary of KCNQ current inhibition at −20 mV (before and after a step to +105 mV) for 4 s ($KCNQ3^{A315T}$ $n = 5$; KCNQ2/3 $n = 4$; KCNQ3/5 $n = 3$). (*c*) Time constants of single-exponential fits to current recovery after Ci-VSP activation ($KCNQ3^{A315T}$ $n = 5$; KCNQ2/3 $n = 4$; KCNQ3/5 $n = 3$). Data represent mean ± SEM. $^*p < 0.05$, using the ANOVA Tukey post hoc test. To see this figure in color, go online.

In the hippocampus, activation of cholinergic fibers leads to inhibition of the sAHP through activation of muscarinic receptors (26–28). Recent work using muscarinic receptor knockout mice showed that M1 muscarinic receptors mediate the effects of acetylcholine in CA3/CA1 pyramidal neuron excitability, including inhibition of the sAHP (29). Activation of M1 muscarinic receptors leads to the activation of Gq-coupled receptors and subsequent activation of phospholipase C, which in turn breaks down $PIP_2$ to generate PKC and DAG (27,28). Although cholinergic receptor agonists potentially can inhibit the sAHP through multiple downstream mechanisms, recent work by Villalobos and colleagues (8) demonstrated that Gq-mediated GPCRs partly inhibit the sAHP through $PIP_2$ depletion. Therefore, we tested whether ablation of KCNQ3 channels increases the sensitivity of the sAHP to muscarinic receptor activation.

We measured the IsAHP in CA3 pyramidal neurons under voltage clamp after a 100 ms depolarization to +45 mV from a holding potential of −55 mV. This depolarization step activates voltage-gated calcium channels. The IsAHP is manifested as a slow-rising and decaying outward current activated by the influx of calcium after the return of the membrane potential to −55 mV (1). In CA3 neurons, this calcium influx also triggers calcium-induced calcium release from internal stores, further prolonging the sAHP (30,31). We recorded the IsAHP in the presence of 100 nM apamin to block calcium-activated SK channels because their deactivation might have overlapped with the IsAHP activation. We did not use blockers for calcium-activated BK or IK channels (the latter of which was recently suggested to be an sAHP channel (32)), as we did not observe any significant inhibition of the sAHP by 100 nM charybdotoxin, a toxin that robustly inhibits both of these channels (Fig. 5).

Previous work in hippocampal and cortical slices has shown that oxotremorine (Oxo) is a partial muscarinic receptor agonist for stimulating phosphoinositide turnover (~20–25% of maximum) (33). Consistent with this, application of Oxo blocked the IsAHP current to 59% ± 5% after 10 min of continuous bath application ($n = 9$) (Fig. 6, *a*, *e*, and *f*). In contrast, we found that Oxo inhibited the IsAHP by 83% ± 5.9% ($n = 7$) in pyramidal neurons from *Kcnq3*-null mice, significantly more than in control mice (Fig. 6, *c*, *e*, and *f*). This result is similar to those obtained in experiments using the full agonist Oxo-M in control slices or using slices from $Pipki\gamma^{+/-}$ mice, which have lower phosphoinositide levels (34). Thus, and consistent with our hypothesis, in the absence of KCNQ3 channels, the remaining KCNQ/IsAHP channels are more susceptible to a $PIP_2$ reduction induced by sustained cholinergic stimulation. However, our data cannot exclude the possibility that the remaining sAHP channels in the *Kcnq3*-null neurons are also more susceptible to kinase or phosphatase signaling activated by muscarinic receptors downstream of $PIP_2$ depletion (35).

We next tested whether KCNQ3-containing channels underlie the sAHP current in *Hpca*-null CA3 pyramidal neurons. Hippocalcin is an sAHP calcium sensor that acts upstream of PIPKIγ, presumably triggering the $PIP_2$ surge that gates the sAHP (1,8). A smaller surge of $PIP_2$ should

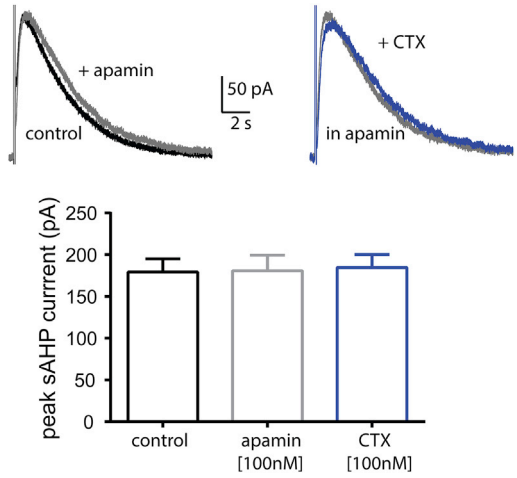


FIGURE 5 BK, SK, and IK channels do not mediate the sAHP current in mouse CA3 pyramidal neurons. Top panel: representative traces from sAHP currents in the presence or absence of the SK channel blocker apamin (100 nM) and in the presence or absence of the BK and IK inhibitor charybdotoxin (CTX; 100 nM). As all sAHP current experiments took place in the presence of apamin, CTX was applied after application of apamin. Bottom panel: summary graph of the sAHP current amplitude in the absence (control $n = 7$) or presence of the BK, SK, and IK inhibitors apamin ($n = 7$) and CTX ($n = 4$). Data represent means ± error of the mean. To see this figure in color, go online.

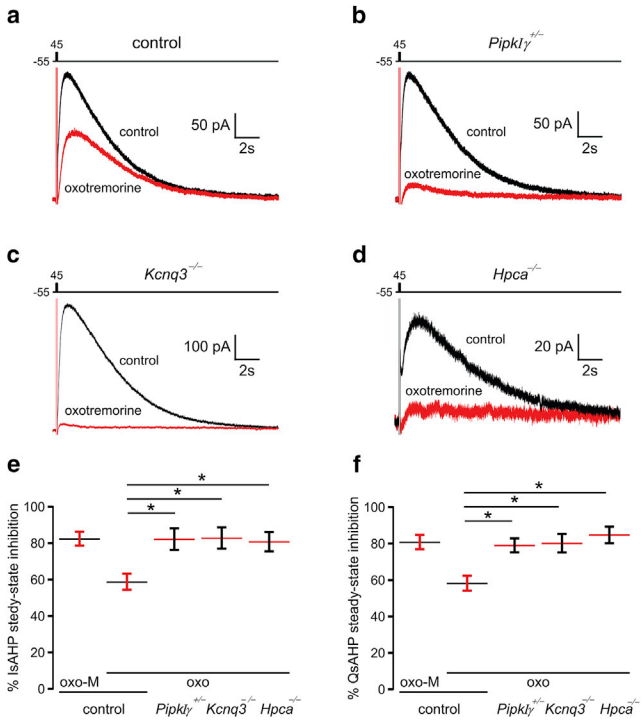


FIGURE 6 Loss of Hpca or KCNQ3 channels increases IsAHP sensitivity to muscarinic activation. Superimposed IsAHP traces before (*black*) and after (*red*) application of 10 $\mu$M of the partial agonist Oxo to (*a*) control pyramidal neurons ($n = 9$), (*b*) *PIPKI*$\gamma$-deficient neurons ($n = 5$), (*c*) *Kcnq3*-null neurons ($n = 7$), and (*d*) *Hpca*-null neurons ($n = 9$). (*e* and *f*) Summary data show the effects of Oxo application on (*e*) IsAHP amplitude and (*f*) charge (sAHP charge (QsAHP); the QsAHP was integrated across 18 s from the peak of the IsAHP) under the different conditions. For comparison, we also include the full agonist Oxo-M (1 $\mu$M; $n = 10$), which blocks the IsAHP and QsAHP. Note that in neurons deficient in PIPKI$\gamma$, KCNQ3, or Hpca, Oxo produces a block similar to Oxo-M in control neurons. Data represent mean $\pm$ SEM. $^*p < 0.05$ using the ANOVA Tukey post hoc test. To see this figure in color, go online.

occur in the absence of hippocalcin, which would explain the diminished amplitude of the IsAHP in *Hpca*-knockout mice (control 253 $\pm$ 11 pA, $n = 17$; $Hpca^{-/-}$ 113 $\pm$ 15 pA, $n = 9$, $p < 0.001$ Student's *t*-test). Such a decrease might also explain the heightened sensitivity of the IsAHP to Oxo inhibition in the *Hpca*-null neurons (81% $\pm$ 5.3%, $n = 9$; Fig. 6, *d–f*). We therefore tested the effect of KCNQ3 ablation on the IsAHP in *Hpca*-null neurons. We would predict that KCNQ3 channels are the predominant $PIP_2$ sensors for gating the IsAHP in these neurons due to their ability to operate under lower $PIP_2$ concentrations. We found that under normal $PIP_2$ conditions, the IsAHP was not diminished in CA3 pyramidal neurons from *Kcnq3*-knockout mice (control: 253 $\pm$11 pA, $n = 17$; *Kcnq3*-null: 304 $\pm$ 21 pA, $n = 21$, $p = 0.052$, Student's *t*-test). However, this lack of an effect on the IsAHP did not appear to be due to an absence of participation of KCNQ3 channels in the sAHP current, as application of retigabine, a modulator of sAHP kinetics (36), had no effect on the sAHP current time course in *Kcnq3*-null neurons (Fig. 7). KCNQ3 channel activation kinetics are sensitive to retigabine (37), even in the presence of elevated $PIP_2$ levels (Fig. 8). Importantly, the IsAHP is nearly eliminated in $Hpca^{-/-}$:$Kcnq3^{-/-}$ double-knockout mice, a presumed $PIP_2$-depleted condition (Fig. 9; $Hpca^{-/-}$ 83 $\pm$ 23 pA, $n = 6$; $Hpca^{-/-}$;$Kcnq3^{-/-}$: 11 $\pm$ 3 pA, $n = 5$, $p < 0.05$). These data support our assertion that KCNQ3-containing channels in pyramidal neurons have an important role in the IsAHP, but primarily under conditions of low $PIP_2$ levels.

## DISCUSSION

The sAHP participates in fundamental neurological processes, and its dysfunction is thought to underlie disorders of neuronal hyperexcitability, such as epilepsy (4). Until

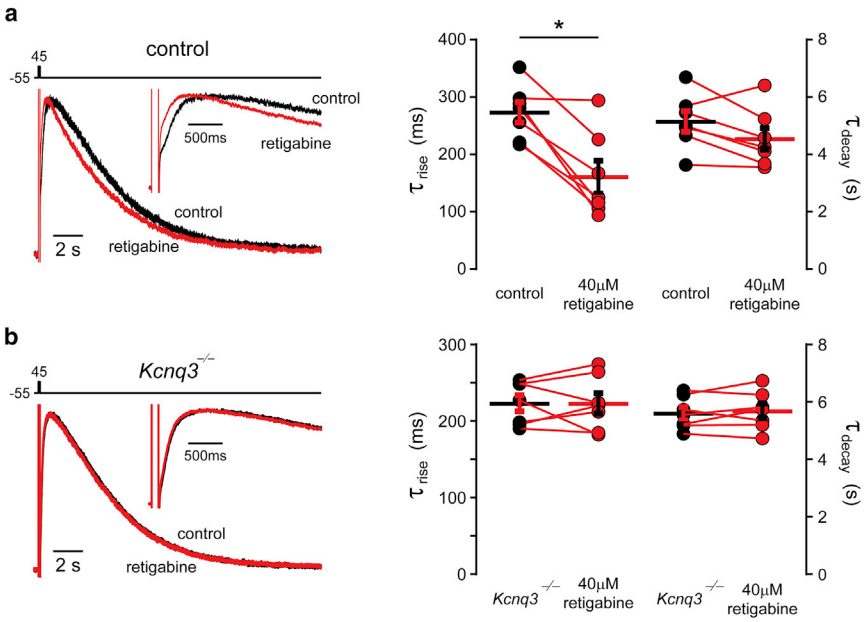


FIGURE 7 KCNQ3 channels are required for retigabine to modulate the IsAHP time course. (*a*) Left: superimposed normalized IsAHP traces before (*black*) and after (*red*) application of 40 $\mu$M retigabine in control pyramidal neurons. Right: summary data showing the effect of retigabine on the activation and decay time constants in control neurons ($n = 7$, $^*p < 0.05$, Student's *t*-test). (*b*) Left: superimposed normalized IsAHP traces before (*black*) and after (*red*) application of 40 $\mu$M retigabine in *Kcnq3*-null pyramidal neurons. Right: summary data showing the effect of retigabine on the activation and decay time constants in *Kcnq3*-null neurons ($n = 7$, $^*p < 0.05$, Student's *t*-test). To see this figure in color, go online.

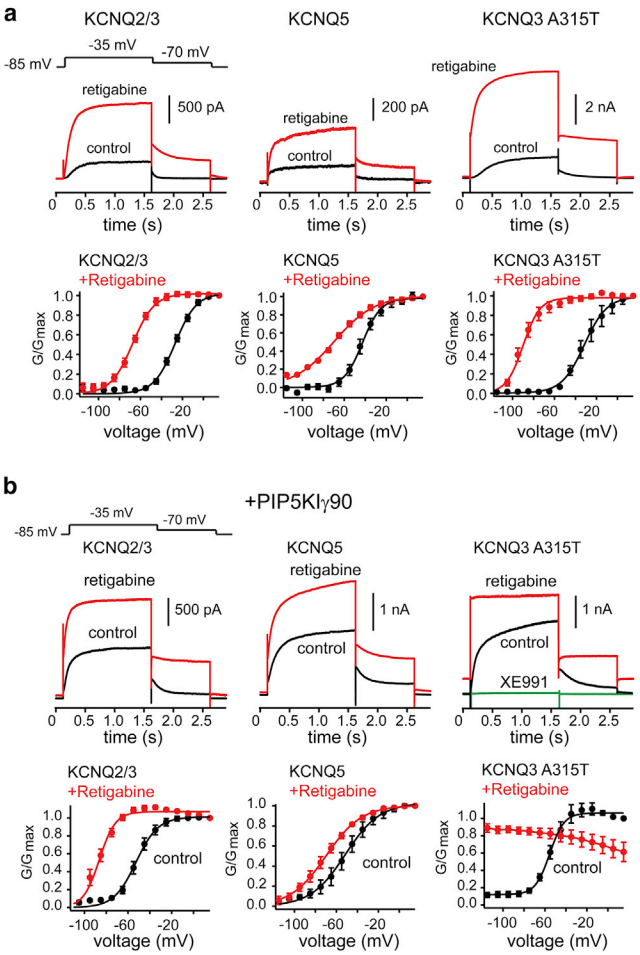


FIGURE 8 PIP2 enhances the effect of retigabine on KCNQ channel voltage activation. For these experiments, KCNQ currents were measured at various test potentials elicited by a 1 s depolarization from −85 mV and were followed by a return step to −70 mV. Test potentials ranged from −115 mV to +15 mV in 10-mV increments. (*a*) Top panels: representative current traces from −85 mV to −35 mV from heterologous cells expressing KCNQ2/3, KCNQ5, and KCNQ3$^{A315T}$ in the absence or presence of 40 $\mu$M retigabine. Bottom panels: summary data of the current-to-voltage relationship of KCNQ2/3 ($n = 8$; $V_{0.5} = -27 \pm 1$ mV, slope factor $= 10 \pm 0.9$; +retigabine $V_{0.5} = -68 \pm 1$ mV, slope factor $= 11 \pm 1$), KCNQ5 ($n = 10$; $V_{0.5} = -43 \pm 2$ mV, slope factor $= 9 \pm 0.9$; +retigabine $V_{0.5} = -67 \pm 2$ mV, slope factor $= 13 \pm 1$), or KCNQ3$^{A315T}$ ($n = 5$; $V_{0.5} = -35 \pm 2$ mV, slope factor $= 9.5 \pm 1$; +retigabine $V_{0.5} = -89 \pm 3$ mV, slope factor $= 8 \pm 2$) in the absence or presence of 40 $\mu$M retigabine. (*b*) Top panels: representative current traces from −85 mV to −35 mV from heterologous cells expressing PIPKIγ90 and either KCNQ2/3, KCNQ5, or KCNQ3$^{A315T}$ in the absence or presence of 40 $\mu$M retigabine. Bottom panels: summary data of the current-to-voltage relationship of KCNQ2/3 ($n = 6$; $V_{0.5} = -52 \pm 2$ mV, slope factor $= 10 \pm 2$; +retigabine $V_{0.5} = -88 \pm 3$ mV, slope factor $= 8 \pm 2$), KCNQ5 ($n = 5$; $V_{0.5} = -54 \pm 6$ mV, slope factor $= 13 \pm 2$; +retigabine $V_{0.5} = -70 \pm 4$ mV, slope factor $= 17 \pm 1$), or KCNQ3$^{A315T}$ ($n = 5$; no fit, just a line through the points) in the presence or absence of retigabine. Data represent means ± error of the mean. To see this figure in color, go online.

recently, the molecular players that shape sAHP activity, and how they give rise to the sAHP, were completely unknown (1). Building on recent findings suggesting that

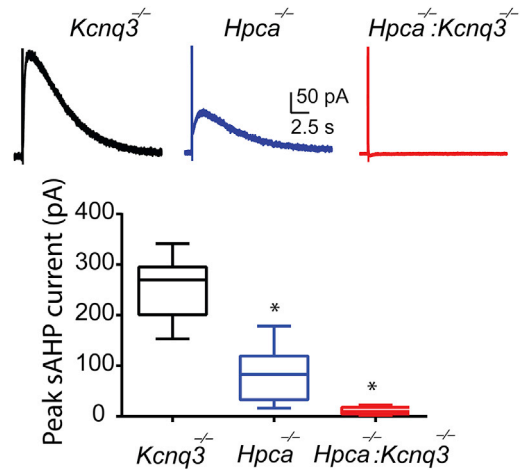


FIGURE 9 KCNQ3 channels mediate the sAHP current in *Hpca*-null neurons. Top: representative sAHP current traces from *Kcnq3*-null ($n = 13$), *Hpca*-null ($n = 6$), or *Hpca*:*Kcnq3*-null ($n = 5$) neurons. Bottom: summary whisker graph showing that the sAHP current is vastly diminished in the absence of both Hpca and KCNQ3 channels. *$p < 0.05$ using the ANOVA Fisher post hoc test. To see this figure in color, go online.

$PIP_2$ gates the sAHP, in this study we show that 1) $PIP_2$ levels determine the voltage-activation properties of KCNQ channels, allowing them to activate within the operating range of the sAHP, and 2) KCNQ3 channels are critical for the sAHP under conditions of low or depleted $PIP_2$ levels. These findings provide new insights into the network of intracellular and membrane-bound signaling mediators that affect the sAHP/IsAHP.

## KCNQ voltage dependence is dynamic and $PIP_2$ dependent

Our data likely resolve the question of how KCNQ channels, which typically activate at membrane potentials positive to −60 mV (19,38), can mediate the (I)sAHP, which is active below −60 mV (1). Recent molecular-dynamics simulations of KCNQ2 channels identified a new $PIP_2$-binding site within the KCNQ2 S4-S5 linker domain (K230 KCNQ2 numbering) (14). This site is conserved across KCNQ3 and KCNQ5 channels. Importantly, disruption of this site changes the KCNQ2 voltage dependence, shifting to more depolarized membrane potentials. The data we obtained using HEK293T cells extend those findings to show that $PIP_2$ regulates the voltage dependence of all cortical KCNQ channels, in addition to its well-characterized ability to increase the KCNQ channel open probability. Importantly, the voltage-activation effects of $PIP_2$ were retained in the presence of the KCNQ channel auxiliary subunit BACE1 (15). Considering that $PIP_2$ is a candidate gating molecule for the (I)sAHP, we surmise that elevated levels of $PIP_2$ can transiently change the KCNQ channel voltage activation and open probability such that they can activate within the operating range of the sAHP.

### KCNQ3 is essential for the sAHP in *Hpca*-null mice

Our data suggest that KCNQ3-containing channels play an important role in maintaining the IsAHP under certain conditions. Importantly, our work demonstrates that KCNQ3 is required to maintain the IsAHP when Hpca is ablated. Hippocalcin is an essential sAHP calcium sensor in pyramidal neurons (5,7,36,39) and is presumed to trigger the $PIP_2$ changes that activate the sAHP (1,8). Consequently, loss of Hpca might lead to smaller $PIP_2$ changes within the vicinity of the sAHP channels after calcium influx. Therefore, in *Hpca*-null neurons, potassium channels with more sensitivity to $PIP_2$ would predominantly mediate the sAHP. Of all the KCNQ channels, KCNQ3 channels have the highest affinity for $PIP_2$-induced increases in open probability (10–12,40), and our data from HEK293T cells demonstrate that they are very sensitive to $PIP_2$-induced leftward shifts in voltage activation. Consistent with this interpretation, there is an almost complete loss of the sAHP current in *Hpca*:*Kcnq3* double-knockout mice.

In contrast to the $KCNQ3^{A315T}$ mutant that we used in this study, wild-type KCNQ3 channels express poorly as homomers in cells. Consequently, it is unlikely that KCNQ3 homomers mediate the sAHP current in *Hpca*-null neurons. The current understanding is that KCNQ3 channels are found as heteromers of KCNQ2/3, and possibly KCNQ3/5, in neurons (18,41). Recent work has also shown that binding of $PIP_2$ solely to KCNQ3 channels is sufficient to open heteromeric KCNQ2/3 channels (11), albeit with low probability. Therefore, we speculate that in *Hpca*-knockout mice, KCNQ3 channels are the main $PIP_2$ sensors leading to activation of KCNQ2/3 or KCNQ3/5 channels. As such, in the absence of KCNQ3 channels in *Hpca*-null neurons, the $PIP_2$ level changes are not sufficient to open the remaining KCNQ2 and KCNQ5 homomeric channels. We should note that KCNQ3 ablation leads to minimal changes in KCNQ2 and KCNQ5 protein levels in the mouse hippocampus.

### KCNQ channels as candidate channels underlying the sAHP

Several lines of evidence indicate that KCNQ channels partly underlie the sAHP: 1) expression of dominant-negative KCNQ2/3 and KCNQ5 channels in CA3 pyramidal neurons decreases the sAHP current (39,43), 2) mice lacking various KCNQ channel subunits have reduced sAHP currents in hippocampal dentate granule cells and dorsal root ganglion neurons (39,42), 3) the KCNQ channel blockers XE991 and UCL2077 inhibit the sAHP in certain neuron populations (16,44), and 4) retigabine, an allosteric modulator that facilitates KCNQ2/3 channel activation, speeds up the sAHP current time course (36). However, the role of KCNQ channels in the sAHP is still debated because none of these manipulations completely eliminates the sAHP current, and because the sAHP current is unaffected in pyramidal neurons from $Kcnq3^{-/-}$ and $Kcnq2^{+/-}$ mice (39). Here, we report, to our knowledge, the first genetic manipulation that largely decreases the sAHP current (~95%) from CA3 pyramidal neurons: simultaneous deletion of KCNQ3 and the sAHP calcium sensor Hpca.

If KCNQ3 does play a role in CA3 pyramidal neurons, why is it that dentate granule cells from *Kcnq3*-null mice have a reduced sAHP current, unlike what is observed in *Kcnq3*-null pyramidal neurons? We suspect that this is the case because dentate granule cells have much lower levels of Hpca compared with pyramidal neurons (45). As a result, dentate granule cells are likely to generate lower levels of $PIP_2$, making them more susceptible to the loss of high-$PIP_2$-affinity KCNQ3 channels than pyramidal neurons. By genetically ablating *Hpca*, pyramidal neurons also become vulnerable to the loss of KCNQ3 channels.

## CONCLUSIONS

In summary, our work strongly supports the notion that KCNQ3 channels play a role in the IsAHP, particularly under conditions of low $PIP_2$ levels. Additionally, our data show that $PIP_2$ can alter the voltage sensitivity of KCNQ channels, suggesting that KCNQ channel voltage activation is dynamic.

## AUTHOR CONTRIBUTIONS

K.S.K., K.M.D., J.M.H., and A.V.T. designed research and analyzed data. K.S.K., K.M.D., and J.M.H. performed research. H.S. contributed analytic tools. K.S.K., K.M.D., and A.V.T. wrote the manuscript.

## ACKNOWLEDGMENTS

We thank Dr. Karen Menuz, Dr. Jacques Wadiche, and members of the A.V.T. lab for discussions and reading the manuscript.

This work was supported by an NIH grant to A.V.T. (NS073981).

## REFERENCES

1. Andrade, R., R. C. Foehring, and A. V. Tzingounis. 2012. The calcium-activated slow AHP: cutting through the Gordian knot. *Front. Cell. Neurosci.* 6:47.
2. Disterhoft, J. F., and M. M. Oh. 2006. Learning, aging and intrinsic neuronal plasticity. *Trends Neurosci.* 29:587–599.
3. Zhang, L., M. Ouyang, …, S. A. Thomas. 2013. The slow afterhyperpolarization: a target of β1-adrenergic signaling in hippocampus-dependent memory retrieval. *J. Neurosci.* 33:5006–5016.
4. McCormick, D. A., and D. Contreras. 2001. On the cellular and network bases of epileptic seizures. *Annu. Rev. Physiol.* 63:815–846.
5. Tzingounis, A. V., M. Kobayashi, …, R. A. Nicoll. 2007. Hippocalcin gates the calcium activation of the slow afterhyperpolarization in hippocampal pyramidal cells. *Neuron.* 53:487–493.
6. Abel, H. J., J. C. Lee, …, R. C. Foehring. 2004. Relationships between intracellular calcium and afterhyperpolarizations in neocortical pyramidal neurons. *J. Neurophysiol.* 91:324–335.

7. Villalobos, C., and R. Andrade. 2010. Visinin-like neuronal calcium sensor proteins regulate the slow calcium-activated afterhyperpolarizing current in the rat cerebral cortex. *J. Neurosci.* 30:14361–14365.
8. Villalobos, C., R. C. Foehring, …, R. Andrade. 2011. Essential role for phosphatidylinositol 4,5-bisphosphate in the expression, regulation, and gating of the slow afterhyperpolarization current in the cerebral cortex. *J. Neurosci.* 31:18303–18312.
9. Delmas, P., and D. A. Brown. 2005. Pathways modulating neural KCNQ/M (Kv7) potassium channels. *Nat. Rev. Neurosci.* 6:850–862.
10. Hernandez, C. C., B. Falkenburger, and M. S. Shapiro. 2009. Affinity for phosphatidylinositol 4,5-bisphosphate determines muscarinic agonist sensitivity of Kv7 K+ channels. *J. Gen. Physiol.* 134:437–448.
11. Telezhkin, V., D. A. Brown, and A. J. Gibb. 2012. Distinct subunit contributions to the activation of M-type potassium channels by PI(4,5)P2. *J. Gen. Physiol.* 140:41–53.
12. Li, Y., N. Gamper, …, M. S. Shapiro. 2005. Regulation of Kv7 (KCNQ) K+ channel open probability by phosphatidylinositol 4,5-bisphosphate. *J. Neurosci.* 25:9825–9835.
13. Hernandez, C. C., O. Zaika, and M. S. Shapiro. 2008. A carboxy-terminal inter-helix linker as the site of phosphatidylinositol 4,5-bisphosphate action on Kv7 (M-type) K+ channels. *J. Gen. Physiol.* 132:361–381.
14. Zhang, Q., P. Zhou, …, H. Yang. 2013. Dynamic PIP2 interactions with voltage sensor elements contribute to KCNQ2 channel gating. *Proc. Natl. Acad. Sci. USA.* 110:20093–20098.
15. Hessler, S., F. Zheng, …, C. Alzheimer. 2015. β-Secretase BACE1 regulates hippocampal and reconstituted M-currents in a β-subunit-like fashion. *J. Neurosci.* 35:3298–3311.
16. Soh, H., and A. V. Tzingounis. 2010. The specific slow afterhyperpolarization inhibitor UCL2077 is a subtype-selective blocker of the epilepsy associated KCNQ channels. *Mol. Pharmacol.* 78:1088–1095.
17. Suh, B. C., and B. Hille. 2007. Electrostatic interaction of internal Mg2+ with membrane PIP2 seen with KCNQ K+ channels. *J. Gen. Physiol.* 130:241–256.
18. Peters, H. C., H. Hu, …, D. Isbrandt. 2005. Conditional transgenic suppression of M channels in mouse brain reveals functions in neuronal excitability, resonance and behavior. *Nat. Neurosci.* 8:51–60.
19. Jentsch, T. J. 2000. Neuronal KCNQ potassium channels: physiology and role in disease. *Nat. Rev. Neurosci.* 1:21–30.
20. Zaika, O., C. C. Hernandez, …, M. S. Shapiro. 2008. Determinants within the turret and pore-loop domains of KCNQ3 K+ channels governing functional activity. *Biophys. J.* 95:5121–5137.
21. Miceli, F., M. R. Cilio, …, F. Bezanilla. 2009. Gating currents from neuronal K(V)7.4 channels: general features and correlation with the ionic conductance. *Channels (Austin).* 3:274–283.
22. Gourgy-Hacohen, O., P. Kornilov, …, Y. Paas. 2014. Capturing distinct KCNQ2 channel resting states by metal ion bridges in the voltage-sensor domain. *J. Gen. Physiol.* 144:513–527.
23. Shapiro, M. S., J. P. Roche, …, B. Hille. 2000. Reconstitution of muscarinic modulation of the KCNQ2/KCNQ3 K(+) channels that underlie the neuronal M current. *J. Neurosci.* 20:1710–1721.
24. Nakajo, K., and Y. Kubo. 2005. Protein kinase C shifts the voltage dependence of KCNQ/M channels expressed in Xenopus oocytes. *J. Physiol.* 569:59–74.
25. Iwasaki, H., Y. Murata, …, Y. Okamura. 2008. A voltage-sensing phosphatase, Ci-VSP, which shares sequence identity with PTEN, dephosphorylates phosphatidylinositol 4,5-bisphosphate. *Proc. Natl. Acad. Sci. USA.* 105:7970–7975.
26. Madison, D. V., B. Lancaster, and R. A. Nicoll. 1987. Voltage clamp analysis of cholinergic action in the hippocampus. *J. Neurosci.* 7:733–741.
27. Dutar, P., and R. A. Nicoll. 1988. Stimulation of phosphatidylinositol (PI) turnover may mediate the muscarinic suppression of the M-current in hippocampal pyramidal cells. *Neurosci. Lett.* 85:89–94.
28. Nicoll, R. A. 1988. The coupling of neurotransmitter receptors to ion channels in the brain. *Science.* 241:545–551.
29. Dasari, S., and A. T. Gulledge. 2011. M1 and M4 receptors modulate hippocampal pyramidal neurons. *J. Neurophysiol.* 105:779–792.
30. Qin, Z., X. Zhou, …, H. H. Chen. 2012. LIM domain only 4 (LMO4) regulates calcium-induced calcium release and synaptic plasticity in the hippocampus. *J. Neurosci.* 32:4271–4283.
31. Tanabe, M., B. H. Gähwiler, and U. Gerber. 1998. L-type Ca2+ channels mediate the slow Ca2+-dependent afterhyperpolarization current in rat CA3 pyramidal cells in vitro. *J. Neurophysiol.* 80:2268–2273.
32. King, B., A. P. Rizwan, …, R. W. Turner. 2015. IKCa channels are a critical determinant of the slow AHP in CA1 pyramidal neurons. *Cell Rep.* 11:175–182.
33. Gonzales, R. A., and F. T. Crews. 1984. Characterization of the cholinergic stimulation of phosphoinositide hydrolysis in rat brain slices. *J. Neurosci.* 4:3120–3127.
34. Voronov, S. V., S. G. Frere, …, G. Di Paolo. 2008. Synaptojanin 1-linked phosphoinositide dyshomeostasis and cognitive deficits in mouse models of Down's syndrome. *Proc. Natl. Acad. Sci. USA.* 105:9415–9420.
35. Krause, M., and P. Pedarzani. 2000. A protein phosphatase is involved in the cholinergic suppression of the Ca(2+)-activated K(+) current sI(AHP) in hippocampal pyramidal neurons. *Neuropharmacology.* 39:1274–1283.
36. Kim, K. S., M. Kobayashi, …, A. V. Tzingounis. 2012. Hippocalcin and KCNQ channels contribute to the kinetics of the slow afterhyperpolarization. *Biophys. J.* 103:2446–2454.
37. Tatulian, L., and D. A. Brown. 2003. Effect of the KCNQ potassium channel opener retigabine on single KCNQ2/3 channels expressed in CHO cells. *J. Physiol.* 549:57–63.
38. Wang, H. S., Z. Pan, …, D. McKinnon. 1998. KCNQ2 and KCNQ3 potassium channel subunits: molecular correlates of the M-channel. *Science.* 282:1890–1893.
39. Tzingounis, A. V., and R. A. Nicoll. 2008. Contribution of KCNQ2 and KCNQ3 to the medium and slow afterhyperpolarization currents. *Proc. Natl. Acad. Sci. USA.* 105:19974–19979.
40. Zhang, H., L. C. Craciun, …, D. E. Logothetis. 2003. PIP(2) activates KCNQ channels, and its hydrolysis underlies receptor-mediated inhibition of M currents. *Neuron.* 37:963–975.
41. Schroeder, B. C., M. Hechenberger, …, T. J. Jentsch. 2000. KCNQ5, a novel potassium channel broadly expressed in brain, mediates M-type currents. *J. Biol. Chem.* 275:24089–24095.
42. King, C. H., E. Lancaster, …, S. S. Scherer. 2014. Kv7.2 regulates the function of peripheral sensory neurons. *J. Comp. Neurol.* 522:3262–3280.
43. Tzingounis, A. V., M. Heidenreich, …, T. J. Jentsch. 2010. The KCNQ5 potassium channel mediates a component of the afterhyperpolarization current in mouse hippocampus. *Proc. Natl. Acad. Sci. USA.* 107:10232–10237.
44. Mateos-Aparicio, P., R. Murphy, and J. F. Storm. 2014. Complementary functions of SK and Kv7/M potassium channels in excitability control and synaptic integration in rat hippocampal dentate granule cells. *J. Physiol.* 592:669–693.
45. Kobayashi, M., T. Masaki, …, K. Takamatsu. 2005. Hippocalcin-deficient mice display a defect in cAMP response element-binding protein activation associated with impaired spatial and associative memory. *Neuroscience.* 133:471–484.